ISSN 1674-1056
http://cpb.iphy.ac.cn
http://iopscience.iop.org/cpb
中国物理 B
Chinese Physics
中国物理
Chinese Physics B

Surface plasmon polaritons at the interface of dielectric and graphene medium using Kerr effect

Bakhtawar, Muhammad Haneef, B A Bacha, H Khan, M Atif

Citation: Chin. Phys. B . 2018, 27(11): 114215. **doi:** 10.1088/1674-1056/27/11/114215

Journal homepage: http://cpb.iphy.ac.cn; http://iopscience.iop.org/cpb

What follows is a list of articles you may be interested in

Surface plasmon polariton waveguides with subwavelength confinement

Longkun Yang(杨龙坤), Pan Li(李盼), Hancong Wang(汪涵聪), Zhipeng Li(李志鹏)

Chin. Phys. B . 2018, 27(9): 094216. **doi:** 10.1088/1674-1056/27/9/094216

Plasmonically induced reflection in metal-insulator-metal waveguides with two silver baffles coupled square ring resonator

Zhi-Dong Zhang(张志东), Lian-Jun Ma(马连俊), Fei Gao(高飞), Yan-Jun Zhang(张彦军), Jun Tang(唐军), Hui-Liang Cao(曹慧亮), Bin-Zhen Zhang(张斌珍), Ji-Cheng Wang(王继成), Shu-Bin Yan(闫树斌), Chen-Yang Xue(薛晨阳)

Chin. Phys. B . 2017, 26(12): 124212. **doi:** 10.1088/1674-1056/26/12/124212

A novel phase-sensitive scanning near-field optical microscope

Wu Xiao-Yu, Sun Lin, Tan Qiao-Feng, Wang Jia

Chin. Phys. B . 2015, 24(5): 054204. **doi:** 10.1088/1674-1056/24/5/054204

Transmission through array of subwavelength metallic slits curved with a single step or multi-step

Wang Ying-Qi, Wang Yan-Hua, Zheng Xian-Hua, Ye Jia-Sheng, Zhang Yan, Liu Shu-Tian

Chin. Phys. B . 2014, 23(3): 034202. **doi:** 10.1088/1674-1056/23/3/034202

Enhanced optical transmission by V-shaped nanoslit in metal film

He Meng-Dong, Ma Wang-Guo, Wang Xin-Jun

Chin. Phys. B . 2013, 22(11): 114201. **doi:** 10.1088/1674-1056/22/11/114201

Surface plasmon polariton at the interface of dielectric and graphene medium using Kerr effect

Bakhtawar[1], Muhammad Haneef[1,†], B A Bacha[2], H Khan[1], and M Atif[1]

[1] *Lab of Theoretical Physics, Department of Physics, Hazara University Mansehra* 21300, *Pakistan*
[2] *Department of Physics, University of Malakand, Dir KP, Pakistan*

(Received 4 June 2018; revised manuscript received 6 August 2018; published online 25 October 2018)

We theoretically investigate the control of surface plasmon polariton (SPP) generated at the interface of dielectric and graphene medium under Kerr nonlinearity. The controlled Kerr nonlinear signal of probe light beam in a dielectric medium is used to generate SPPs at the interface of dielectric and graphene medium. The positive, negative absorption, and dispersion properties of SPPs are modified and controlled by the control and Kerr fields. A large amplification (negative absorption) is noted for SPPs under the Kerr nonlinearity. The normal/anomalous slope of dispersion and propagation length of SPPs is modified and controlled with Kerr nonlinearity. This leads to significant variation in slow and fast SPP propagation. The controlled slow and fast SPP propagation may predict significant applications in nano-photonics, optical tweezers, photovoltaic devices, plasmonster, and sensing technology.

Keywords: surface plasmon polariton, Kerr nonlinearity, graphene

PACS: 42.65.–k, 42.50.–p, 42.50.Nn, 42.65.Hw **DOI:** 10.1088/1674-1056/27/11/114215

1. Introduction

The study of light matter interaction at microscopic scale has received enormous attention of the researchers.[1–8] The study of optical phenomena related to the electromagnetic response of metals has been recently termed as plasmonics or nanoplasmonics. This rapidly growing field of nanoscience is mostly concerned with the control of optical radiation on the subwavelength scale. A plasmon is a collective oscillation of free electrons which leads to characteristic energy losses in metals.[9] The work of Wood in 1902 provided the very first scientific study for the presence of surface plasmon on metallic grating in optical reflection measurements.[10] The existence of surface plasmon wave was first predicted by Ref. [11] in a transversemagnetic (TM) mode. Surface plasmon polariton (SPP) modes are two-dimensional bounded excitations, guided by the surface whose electromagnetic field decays exponentially with distance from the surface.[12] SPPs possess remarkable capabilities of concentrating light in a nanoscale region, which leads to an enhancement of electromagnetic field at the interface,[13] resulting in an extraordinary sensitivity of SPPs to surface conditions. Surface related phenomena including surface roughness and adsorbates on surface are well described by using this sensitivity.[12] Several optical demonstrations, such as well defined optical transmission, huge field enhancement, and negative refraction are the contributions of SPPs in metals at subwavelength scale.[14] Surface-enhanced optical phenomena, such as Raman scattering, second harmonic generation (SHG), and fluorescence are the consequences of significant enhancement of localized field.[15–19]

SPPs can be excited by an incident electromagnetic wave if their wavelength vectors match. What distinguishes SPPs from photons is that they have a much smaller wavelength at the same frequency.[20] Scanning near-field optical microscopy (SNOM)[21] provides an opportunity to probe the SPP field directly over a surface in nanometer range. The implementation of SNOM has led to a breakthrough in surface polariton studies.[22–29] Surface plasmon polariton scattering, interference, backscattering, and localization have been visualized and investigated directly on the surface.[28,29]

In recent years, there has been a rapid expansion of research into metasurfaces to achieve an efficient control over the parameters of nonlinear optical interactions, which leads to the fabrication of tunable optical devices. The nonlinear response of a material is sensitive to the field localization within nanostructure. Therefore, efficient control over different nonlinear optical properties can be achieved by varying the shape anisotropy and geometry of a particular metasurface (plasmonic metamaterials). Intensity, phase, and state of polarization are different parameters which can be used for calculating nonlinear optical response. To achieve active functionality, one must include nonlinearity into metasurface design,[30] by using either the nonlinearity of plasmonic material itself[31,32] or by incorporating high nonlinear material such as semiconductor quantum wells combined with existing plasmonic metasurface structure.[33,34] Kerr nonlinearity, corresponding to the refractive part of the third-order susceptibility, results in an intensity-dependent refractive index. The intense laser pulses in Kerr nonlinearity lead to several important phenomena such as self-focusing,[35] optical phase conjugation,[36] optical bistability,[37] and two beam coupling.[38]

†Corresponding author. E-mail: haneef.theoretician@gmail.com

© 2018 Chinese Physical Society and IOP Publishing Ltd

Many proposals have been suggested for achieving enhanced Kerr nonlinearity accompanied with negligible absorption. Sahraia *et al.*[39] described the Kerr nonlinearity and optical multi-stability in a four level Y-type atomic system. Schmidt studied Kerr nonlinearity in light propagation and observed enhancement in the Kerr nonlinearity to several orders of magnitude.[40] Bacha *et al.*[41] used Kerr nonlinearity for enhancement of superluminality and practical application of temporal cloaking. Quantum sized gold film provides a promising sensing platform for metasurfaces due to its giant optical nonlinearity. By varying the incident optical power through quantum sized gold film, the active functionality of the material can be determined. At low power region, the device acts as a normal reflecting surface. It becomes a phase grating when the incident power is high enough and enhances the nonlinear response.[42] Rokhsari and his co-workers[43] developed an experimental technique for observation of optical Kerr effect in microcavities at room temperature. At this stage one can raise some questions. Can SPP waves be generated from the control output pulse of dielectric? How the Kerr instability in dielectric be used for wide band optical amplification? Can the SPPs be controlled by utilizing large optical nonlinearities such as Kerr nonlinearity? What will be the nonlinear response to the applied fields at the interface of dielectric and graphene medium? To resolve these issues, we consider a four level dielectric atomic system and a graphene medium for describing the dynamics of light pulses in Kerr nonlinear media. By using control fields and Kerr nonlinearity, the positive and negative absorption of SPPs is investigated. The normal anomalous dispersive properties and propagation length of SPPs are controlled and modified with Kerr nonlinearity. We have noted significant enhancement in the speed of slow and fast propagating plasmon polariton waves.

2. Model of the atomic system

A four level atomic configuration of a dielectric medium and graphene medium is shown in Fig. 1. The dielectric atomic system is shown on dielectric surface. The probe field $E_{\rm p}$ which has Rabi frequency $\Omega_{\rm p}$ is coupled between states $|2\rangle$ and $|4\rangle$. The $|1\rangle$ and $|4\rangle$ are coupled with control field E_3 having Rabi frequency Ω_3. The $|2\rangle$ and $|3\rangle$ are coupled with a control field E_4 having Rabi frequency Ω_4. The four energy levels of graphene are shown on the graphene surface. In this configuration, probe field $E_{\rm p}$ which has Rabi frequency $\Omega_{\rm p}$ is coupled between states $|1\rangle$ and $|4\rangle$. The control fields E_1 and E_2 with Rabi frequencies Ω_1 and Ω_2 are coupled to states $|2\rangle \Leftrightarrow |3\rangle$ and $|3\rangle \Leftrightarrow |4\rangle$, respectively. The surface plasmon polariton waves are generated at the interface, as shown in Fig. 1. The self Hamiltonian of dielectric system is

$$H_0 = \sum_{i=1}^{4} \hbar\omega_i |i\rangle\langle i|. \tag{1}$$

The Hamiltonian in the interaction picture for dielectric medium of the four level atomic system is written as

$$\begin{aligned} H_{1\rm I} = & -\frac{\hbar}{2}[\Omega_3 {\rm e}^{-{\rm i}\Delta_3 t}|1\rangle\langle 4| + \Omega_{\rm p}{\rm e}^{-{\rm i}\Delta_{\rm pd}t}|2\rangle\langle 4| \\ & + \Omega_4 {\rm e}^{-{\rm i}\Delta_4 t}|2\rangle\langle 3|] + {\rm H.c.} \end{aligned} \tag{2}$$

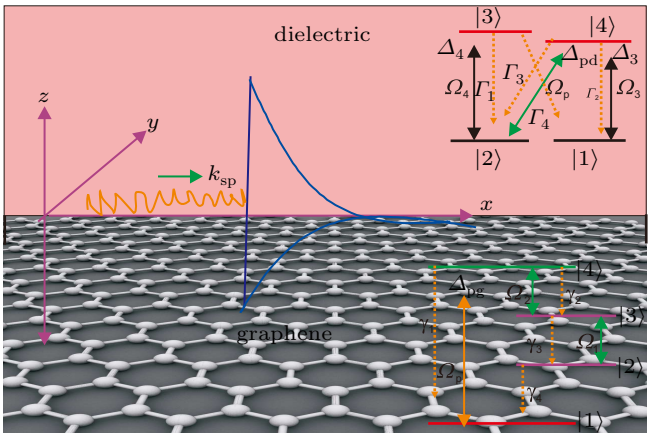


Fig. 1. (color online) Energy diagram of the four level atomic system.

The Hamiltonian in the interaction picture for graphene medium of the four level atomic system is written as

$$\begin{aligned} H_{2\rm I} = & -\frac{\hbar}{2}[\Omega_1 {\rm e}^{-{\rm i}\Delta_1 t}|2\rangle\langle 3| + \Omega_{\rm p}{\rm e}^{-{\rm i}\Delta_{\rm pg}t}|1\rangle\langle 4| \\ & + \Omega_2 {\rm e}^{-{\rm i}\Delta_2 t}|2\rangle\langle 3|] + {\rm H.c.} \end{aligned} \tag{3}$$

The detuning of these fields is related to their corresponding angular frequencies and also to the resonance frequencies of the atomic states, which is given in the following: $\Delta_1 = \omega_{23} - \omega_1$, $\Delta_2 = \omega_{34} - \omega_2$, $\Delta_{\rm pg} = \omega_{14} - \omega_{\rm p}$, and $\Delta_3 = \omega_{14} - \omega_2$, $\Delta_4 = \omega_{23} - \omega_4$, $\Delta_{\rm pd} = \omega_{24} - \omega_{\rm p}$. The master equation for density matrix is given below

$$\rho = -\frac{\rm i}{\hbar}[\rho, H_{(1,2)\rm I}] - \frac{1}{2}\Gamma_{ij}\sum(\sigma^\dagger\sigma\rho + \rho\sigma^\dagger\sigma - 2\sigma\rho\sigma^\dagger), \tag{4}$$

where $\sigma^\dagger$ is the raising operator and σ is the lowering operator for the atomic decays. Here, $\Omega_{\rm p}$ is taken in the first order, while $\Omega_{1,2,3,4}$ are taken in all order of perturbations. The atoms are initially assumed to be in the ground state $|2\rangle$ in dielectric medium, and in the ground state $|1\rangle$ in graphene medium. Using master Eq. (4), the systems are solved for the equation of motion. We solved sixteen density matrix equations. Furthermore, the coupled rate equations are considered out of sixteen density matrix in the explicitly time independent form. The first order perturbation conditions and initial population conditions are $\widetilde{\rho}_{11}^{(0)} = 1$ for dielectric and $\widetilde{\rho}_{22}^{(0)} = 1$ for graphene medium. $\widetilde{\rho}_{33}^{(0)} = \widetilde{\rho}_{44}^{(0)} = \widetilde{\rho}_{ij}^{(0)} = 0$ are applied to the coupled rates equation. The following expression is used for the solution of $\widetilde{\rho}_{24}^{(1)}$ and $\widetilde{\rho}_{14}^{(1)}$ for dielectric and graphene systems:

$$Z(t) = \int_{-\infty}^{t} {\rm e}^{-A(t-t')}B{\rm d}t' = A^{-1}B. \tag{5}$$

In the above equation, $Z(t)$ and B are column matrices while A is an $n\times n$ matrix. Equation (5) is solved for the systems to first order and the following density matrix is obtained as:

$$\widetilde{\rho}_{24} = -\frac{2\mathrm{i}(A_3|\Omega_3|^2 + A_2(4A_3A_4 + |\Omega_4|^2))\Omega_\mathrm{p}}{G + 2(2A_1A_2 + 2A_3A_4 - |\Omega_3|^2)|\Omega_4|^2 + |\Omega_4|^4}, \quad (6)$$

$$\widetilde{\rho}_{14} = \frac{\mathrm{i}[\Omega_\mathrm{p}(B_1B_2 + \frac{1}{4}|\Omega_1|\Omega_2|\mathrm{e}^{\mathrm{i}(\varphi_1-\varphi_2)}]}{2(B_1B_2B_3 + \frac{1}{4}|\Omega_1|\Omega_2|\mathrm{e}^{\mathrm{i}(\varphi_1-\varphi_2)} + \frac{B_1|\Omega_2|^2}{4})}, \quad (7)$$

where

$$A_1 = \mathrm{i}\Delta_\mathrm{pd} - \frac{1}{2}(\Gamma_1 + \Gamma_3), \quad (8)$$

$$A_2 = \mathrm{i}(\Delta_\mathrm{pd} - \Delta_4) - \frac{1}{2}(\Gamma_1 + \Gamma_2 + \Gamma_3 + \Gamma_4), \quad (9)$$

$$A_3 = \mathrm{i}(\Delta_\mathrm{pd} - \Delta_3), \quad (10)$$

$$A_4 = \mathrm{i}(\Delta_\mathrm{pd} - \Delta_4 - \Delta_3) - \frac{1}{2}(\Gamma_1 + \gamma_2 + \gamma_4), \quad (11)$$

$$B_1 = \mathrm{i}(\Delta_\mathrm{pg} - \Delta_2 - \Delta_1) + \frac{1}{2}(\Gamma_1 + \Gamma_4), \quad (12)$$

$$B_2 = \mathrm{i}(\Delta_\mathrm{pg} - \Delta_2) + \frac{1}{2}(\gamma_1 + \gamma_2 + \gamma_4), \quad (13)$$

$$B_3 = \mathrm{i}\Delta_\mathrm{pg} + \frac{1}{2}(\gamma_1 + \gamma_4), \quad (14)$$

$$G = (4A_1A_3 + |\Omega_3|^2)(4A_2A_4 + |\Omega_3|^2). \quad (15)$$

To introduce Kerr effect, $\widetilde{\rho}_{24}$ and $\widetilde{\rho}_{14}$ are expanded in the following way of perturbation limit as:[44]

$$\rho^{(k)}_{14,24} = \rho^{(0)}_{14,24} + I\frac{\partial\rho^{(k)}_{14,24}}{\partial I}. \quad (16)$$

In the case of self Kerr nonlinearity, the susceptibility is taken in the third order form (χ^3) having a unit of $\mathrm{V}^2/\mathrm{m}^2$. The cross Kerr nonlinearity is not due to the probe field intensity, but to the intensity of any other control field. To introduce cross Kerr nonlinearity, Bacha *et al.*[44,45] and Agarwal used Eq. (16), where $I = |\Omega_{1,3}|^2$.

The nonlinearity Kerr susceptibility χ^3 is taken in the order of 3 in self Kerr nonlinearity with a unit of $\mathrm{V}^2/\mathrm{m}^2$. In this case, we produce cross Kerr nonlinearity in the given medium, which is due to the other control field not due probe field himself by the method of Bacha *et al.*,[44,45] and its unit is also $\mathrm{V}^2/\mathrm{m}^2$.

The simplified forms are calculated as

$$\rho^{(k)}_{14} = \frac{\mathrm{i}\Omega_\mathrm{p}B_1B_2}{2(B_1B_2B_3 + \frac{B_1|\Omega_2|^2}{4})} - \frac{\mathrm{i}\Omega_\mathrm{p}B_3|\Omega_1|^2|\Omega_2|^4\mathrm{e}^{2\mathrm{i}(\varphi_1-\varphi_2)}}{B_1^2(B_2B_3 + |\Omega_2|^2)^3}, \quad (17)$$

$$\rho^{(k)}_{24} = \frac{-2\mathrm{i}\Omega_\mathrm{p}A_2(4A_3A_4 + |\Omega_4|^2)}{16A_1A_2A_3A_4 + 2(A_1A_2 + A_3A_4)|\Omega_4|^2 + |\Omega_4|^4} + |\Omega_3|^2\left[\frac{(8\mathrm{i}A_2^2A_4 - 2\mathrm{i}(2A_2 + A_3)|\Omega_4|^2)\Omega_\mathrm{p}}{(4A_1A_2 + |\Omega_4|^2)^2(4A_3A_4 + |\Omega_4|^2)}\right]. \quad (18)$$

The Kerr field effected susceptibility is then calculated as follows:

$$\chi_1 = \frac{2N\rho_{24}^2}{\varepsilon_0\hbar\Omega_\mathrm{p}}\widetilde{\rho}^{(k)}_{24}, \quad (19)$$

$$\chi_2 = \frac{2N\rho_{14}^2}{\varepsilon_0\hbar\Omega_\mathrm{p}}\widetilde{\rho}^{(k)}_{14}. \quad (20)$$

The dispersion relation for surface plasmon polaritron is written as

$$k_\mathrm{sp} = \sqrt{\frac{(1+4\pi(\chi_1))(1+4\pi(\chi_2))}{2+4\pi(\chi_1+\chi_2)}}, \quad (21)$$

where $k_\mathrm{sp} = k_0 n_\mathrm{sp}$. The phase velocity of plasmon polariton is written as $v_\mathrm{p} = c/n_\mathrm{r}^\mathrm{sp}$. The intensity of SPPs decreases exponentially along the interface of dielectric and graphene medium with the propagation length L_x as $\mathrm{e}^{-2k_\mathrm{sp}L_x}$. The propagation length of surface plasmon polariton is written as $L_x = 1/2\mathrm{Im}(k_\mathrm{sp})$.

The input light pulse is taken in a Gaussian form as

$$S_\mathrm{i}(t,x) = \exp\left[\frac{(x-ct)^2}{2\tau_0^2c^2} - \mathrm{i}\omega_0 t + \mathrm{i}\frac{\omega_0 t}{c}\right]. \quad (22)$$

The surface plasmon polariton pulse propagating at the interface is the fourier transform of $(S^\mathrm{g}_\mathrm{out}(\omega,x) + S^\mathrm{d}_\mathrm{out}(\omega,x))\exp(\mathrm{i}(k_\mathrm{sp}(\omega)x - \omega_\mathrm{sp}t))$, where $S^\mathrm{g}_\mathrm{out}(\omega,x)$ and $S^\mathrm{d}_\mathrm{out}(\omega,x)$ are the output pulses of graphene and dielectric to the interface in frequency domain, while $\omega_\mathrm{sp} = \omega_\mathrm{p}\sqrt{1/(1+\varepsilon_\mathrm{d})}$, $n_\mathrm{r} = \sqrt{\varepsilon_\mathrm{d}}$, $\omega_\mathrm{p}^2 = \omega^2 - c^2k_\mathrm{sp}^2$. The plasmon polariton pulse in space time domain is written by

$$S_\mathrm{sp}(x,t) = \int_{-\infty}^{\infty} u(x,t)\psi_1(x)\exp\left[-\mathrm{i}\sqrt{\frac{\omega^2(1-(n_\mathrm{r}^\mathrm{sp})^2)}{1+(n_\mathrm{r}^\mathrm{d})^2}} \times\left(\frac{x-ct}{c}\right)\right]\mathrm{d}\omega, \quad (23)$$

where

$$u(x,\omega) = \exp\left[\mathrm{i}\left(-t\omega + \frac{n_\mathrm{r}^\mathrm{g}x\omega}{c}\right)\right] + \exp\left[\mathrm{i}\left(-t\omega + \frac{n_\mathrm{r}^\mathrm{d}x\omega}{c}\right)\right],$$

and

$$\psi_1(x) = \tau_0\exp\left[-\frac{(-1+c)\omega_0(2\mathrm{i}x + (-1+c)\tau_0^2\omega_0)}{2c^2}\right],$$

where n_r^d is the refractive index of dielectric, n_r^g is the refractive index of graphene, and n_r^sp is the refractive index of SPPs.

3. Results and discussions

The results are presented for real and imaginary parts of dispersion relation of surface plasmon polariton (k_sp) under Kerr nonlinearity. The real part of k_sp is related to the dispersion, and the imaginary part is related to the absorption spectrum of surface plasmon polariton. The atomic decay rate γ of dielectric and graphene medium is assumed to be 36.1 MHz,

and other parameters are scaled to this decay rate γ. The parameters $\hbar$, μ_0, and ε_0 are taken as 1 in atomic units. The input pulse width τ_0 is chosen as 10 μs.

In Fig. 2(a), the plots are traced for real and imaginary parts of k_{sp} under Kerr field effect with probe detuning of graphene atomic system, whereas phases $\varphi_{1,2} = \pi/2, \pi/6$ of the control fields $E_{1,2}$ are fixed. The imaginary part is related to the absorption properties of k_{sp}, which has a negative value with probe detuning of graphene energy system. The negative absorption shows amplification of the plasmon polariton pulses. The slope of dispersion has symmetrically normal and anomalous behavior about the resonance point $\Delta_{pg} = 0\gamma$. This shows slow and fast pulse propagation of the surface plasmon polariton under Kerr nonlinearity. Figure 2(b) shows the plots for real and imaginary parts of k_{sp} with probe detuning of dielectric atomic system and in the presence of Kerr nonlinearity. Again, the phases $\varphi_{1,2} = \pi/2, \pi/6$ of the control fields $E_{1,2}$ are kept constant. At the resonance frequency ($\Delta_{pd} = 0\gamma$), the negative absorption peak is large. Furthermore, far from the resonance point there are two positive peaks of absorption, which shows that plasmon pulses rapidly decay at probe detuning of $\pm\Delta_{pd}$. The dispersion is kink and anti kink behavior and show alternate subluminal and superluminal propagation of SPPs.

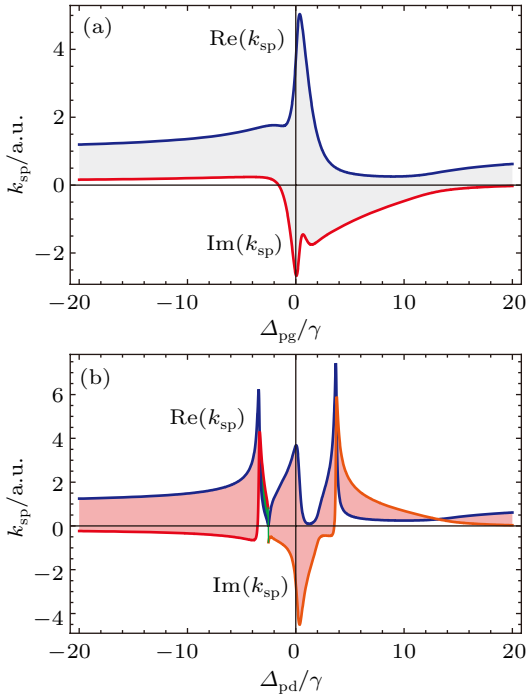


Fig. 2. (color online) Dispersion relation of surface plasmon, while $\gamma_{1,2,3,4} = 1\gamma$, $\Gamma_{1,2,3,4} = 1\gamma$, $\Delta_{1,2} = 0\gamma$, $|\Omega_{1,2,3,4}| = 5\gamma$, $\varphi_{1,2} = \pi/2, \pi/6$, and (a) $\Delta_{pd} = 0\gamma$, (b) $\Delta_{pg} = 0\gamma$.

In Fig. 3(a), the plots are traced for real and imaginary parts of k_{sp} under Kerr field effect with probe detuning of graphene atomic system, and with constant phases $\varphi_{1,2} = \pi/3, \pi/4$ of the control fields $E_{1,2}$. In this case, the absorption is negative with probe detuning Δ_{pg} and largely enhanced near the resonance point at positive detuning. The slope of dispersion is anomalous at this region, which shows superluminal propagation of SPPs. Figure 3(b) shows the plots for real and imaginary parts of k_{sp} in the presence of Kerr field effect with probe detuning of dielectric atomic system, while phases $\varphi_{1,2} = \pi/3, \pi/4$ of the control fields $E_{1,2}$ are constant. The negative absorption symmetric dispersion of positive and negative slope is measured in this case, which shows slow and fast plasmon polariton pulse propagation.

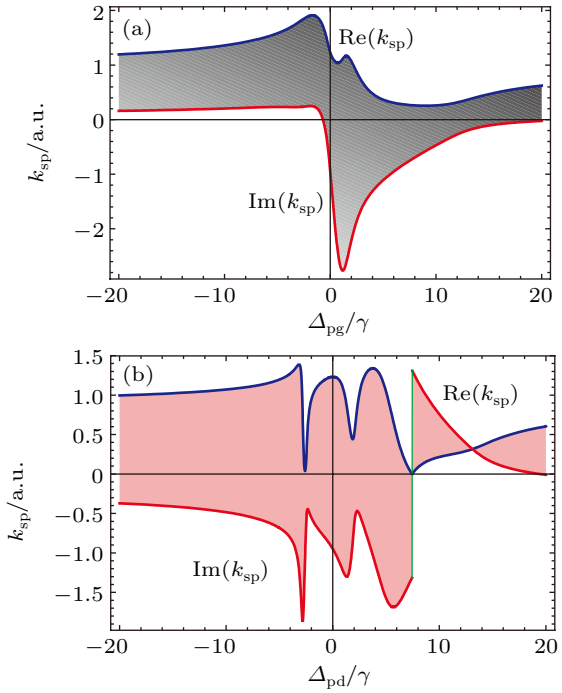


Fig. 3. (color online) Dispersion relation of surface plasmon, while $\gamma_{1,2,3,4} = 1\gamma$, $\Gamma_{1,2,3,4} = 1\gamma$, $\Delta_{1,2} = 0\gamma$, $|\Omega_{1,2,3,4}| = 5\gamma$, $\varphi_{1,2} = \pi/3, \pi/4$, and (a) $\Delta_{pd} = 0\gamma$, (b) $\Delta_{pg} = 0\gamma$.

In Figs. 4(a) and 4(b), the plots are traced for real and imaginary parts of k_{sp} in the presence of Kerr field effect with control field Rabi frequencies $\Omega_{2,4}$, while phases $\varphi_{1,2} = \pi/3, \pi/4$ of the control fields $E_{1,2}$ are kept constant. In Fig. 4(a), the absorption is positive at a very small value of Ω_2. As the value of Ω_2 increases, the absorption becomes negative. The maximum of the negative absorption (amplification) occurs at $\Omega_2 = 4.5\gamma$. Furthermore, when the Rabi frequency of the control field increases from $\Omega_2 = 4.5\gamma$, the negative absorption decreases and again it turns into a positive value. The points $\Omega_2 = 3.2\gamma$ and $\Omega_2 = 8.1\gamma$ are the swamping points from positive to negative and from negative to positive absorption of SPPs, respectively. Figure 4(b) shows real and imaginary parts of k_{sp} which are plotted with the Rabi frequency Ω_4 of the control field E_4 and in the presence of Kerr field effect. The phases $\varphi_{1,2} = \pi/3, \pi/4$ are fixed. A negative absorption peak is noted at $\Omega_4 = 4\gamma$. The slope of dispersion is found normal in this region of the control field Rabi frequency. In this peak region, the negative absorption decreases and the slope becomes more steeper, which rapidly enhances the slow plasmon polariton.

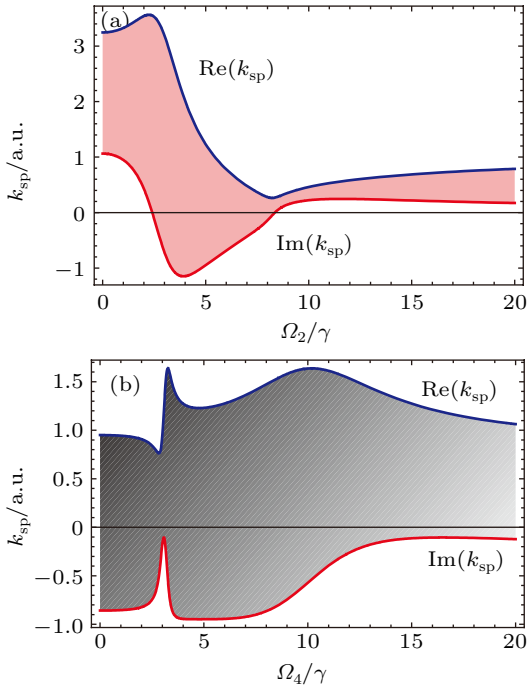


Fig. 4. (color online) Dispersion relation of surface plasmon, while $\gamma_{1,2,3,4} = 1\gamma$, $\Gamma_{1,2,3,4} = 1\gamma$, $\Delta_{1,2} = 0\gamma$, $\varphi_{1,2} = \pi/3, \pi/4$, $\Delta_{\text{pd,pg}} = 0\gamma$, and (a) $|\Omega_{1,3,4}| = 5\gamma$, (b) $|\Omega_{1,2,3}| = 5\gamma$.

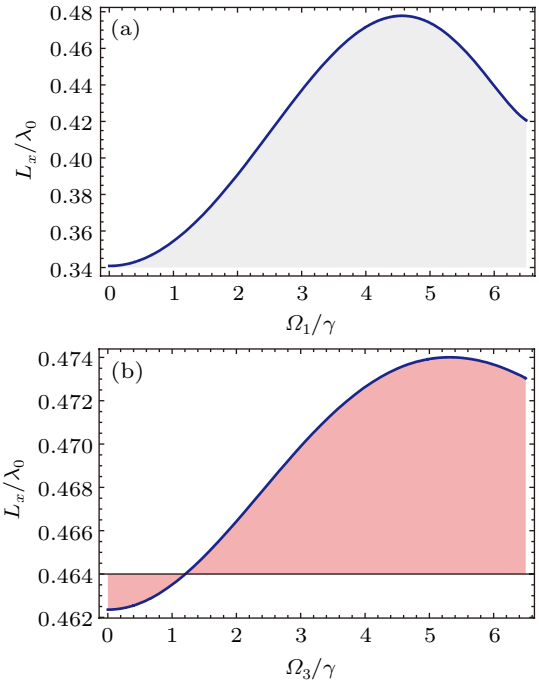


Fig. 5. (color online) Propagation length of surface plasmon in centimeter, while $\gamma_{1,2,3,4} = 1\gamma$, $\Gamma_{1,2,3,4} = 1\gamma$, $\Delta_{1,2} = 0\gamma$, $\varphi_{1,2} = \pi/3, \pi/4$, $\Delta_{\text{pd}} = 0\gamma$, and (a) $|\Omega_{2,3,4}| = 5\gamma$, (b) $|\Omega_{1,2,4}| = 5\gamma$,

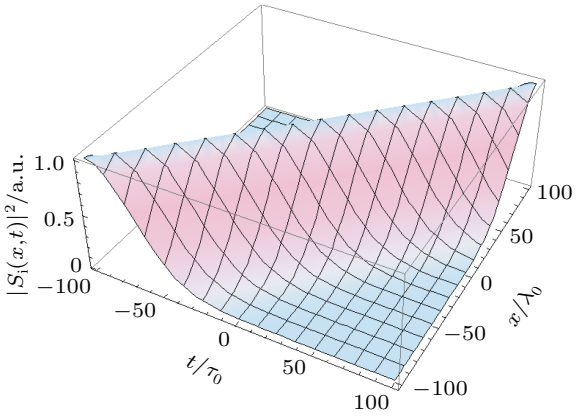


Fig. 6. (color online) Plasmon polariton pulse amplitude versus space time coordinates (x, t), $\tau_0 = 10$ μs.

Figure 5 shows the propagation length of SPPs in the unit of $\lambda_0 = 2\pi c/\omega$ with Kerr field Rabi frequencies $\Omega_{1,3}$, where $\omega = 1000\gamma$ and $c = 3 \times 10^8$ m/s. The y-coordinate is taken as L_x/λ_0, and the propagation length varies with λ_0 in the y-coordinate. Further, the x-coordinate is normalized with γ. The Rabi frequency varies with γ multiplied by the fraction of x-coordinate (thanks to reviewer's comments). The fractional change L_x/λ_0 varies from 0.34 to 0.48 in Fig. 5(a), and from 0.462 to 0.474 in Fig. 5(b) with $|\Omega_{1,3}| = (0\text{–}5)\gamma$. The propagation length L_x varies from $0.34\lambda_0$ to $0.48\lambda_0$ in Fig. 5(a), and $0.462\lambda_0$ to $0.474\lambda_0$ in Fig. 5(b). The intensity of SPPs decreases exponentially along the interface of dielectric and graphene medium. The propagation length of surface plasmon polariton, $L_x = 1/2\text{Im}(k_{sp})$, initially increases with Kerr field Rabi frequency and reaches its maximum value at $|\Omega_{1,3}| = 5\gamma$, then decreases as the Kerr field intensity increases from $|\Omega_{1,3}| = 5\gamma$. The nonlinear effects depend on the propagation length of the SPPs.

Figure 6 shows the input laser pulse which propagates both to dielectric and graphene medium. The input pulse is a Gaussian form in space time domain. The input pulse width in time domain is taken as $\tau_0 = 10$ μs. The input Gaussian pulse is modified with the applications of control fields. The Kerr field as well as the control field significantly changes the property of input pulse within the dielectric and graphene media. The SPPs cannot be excited directly by ordinary probe laser light due to momentum mismatch between the incident light and the SPPs. The electron energy loss spectroscopy, Kretchmann geometry, Otto geometry, metallic grating, and nanoslits are the special designed techniques to excite SPPs by direct light beams. The intensity of the incident Gaussian pulse beam is more significant under these conditions of special excitation geometry. A strong nonlinear response from optically thin structures requires much stronger light–matter interactions than those that are naturally available in bulk nonlinear media. The surface plasmons existing at graphene–dielectric interfaces confine strong field and are efficient to enhance light–matter interactions at the graphene boundary. Plasmonic metasurfaces open new possibilities for nonlinear signal generation. Plasmonic waves enhance the efficiency of nonlinear generation. Any graphene surface can virtually support a nonlinear response, because the electrons at the surface reside in a non-symmetric environment, and can therefore avoid the symmetry constraints. The intrinsic bulk nonlinearity emits nonlinear signals from the surface. To achieve symmetry breaking for SHG metasurfaces, plasmonic nanostructure is used with removed inversion symmetry.[46]

Figure 7 shows the normalized SPP wave intensity $|S_{sp}(x,t)|^2$ at the interface of graphene and dielectric in space time domain in atomic unit. The longer the propagation length, the more interactions with the material, and the greater the nonlinear effects. On the other hand, if the power decreases while the SPPs travel along the optical plasmas at the interface, the effects of nonlinearity diminish. The pulse shape is distorted due to group velocity dispersion $\partial n_g^{sp}/\partial\omega$ and the energy loss of SPPs. The intensity of SPP waves exponentially decays from negative to positive time domain. The intensity along the negative x-coordinate is zero and gradually increases to 4 a.u. (a.u. is short for atomic units), and then exponentially decays to 0.5 a.u.; further, the intensity is again enhanced by the new excitation of SPP waves.

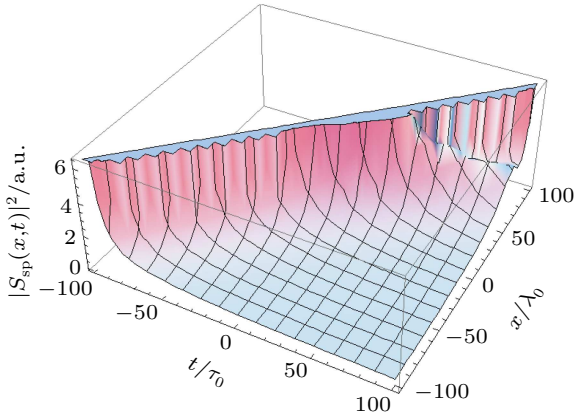


Fig. 7. (color online) Surface plasmon polariton pulse amplitude vs space time coordinates (x,t), while $\gamma_{1,2,3,4} = 1\gamma$, $\Gamma_{1,2,3,4} = 1\gamma$, $\Delta_{1,2} = 0\gamma$, $|\Omega_{1,2,3,4}| = 5\gamma$, $\varphi_{1,2} = \pi/3, \pi/4$, $\Delta_{pd} = 0\gamma$, and $\tau_0 = 10$ μs.

4. Conclusion

In conclusion, the surface plasmon polariton generated at the interface of dielectric and graphene medium is controlled and modified under the effect of Kerr nonlinearity. The output pulse from dielectric and graphene is used to generate surface plasmon polariton. The positive and negative absorption of SPPs with control fields and Kerr nonlinearity is measured. The normal anomalous dispersive properties and propagation length of SPPs are controlled and modified with Kerr nonlinearity. We obtain significant enhancement in the speed of slow and fast propagating plasmon polariton waves. The propagation length L_x varies from $0.34\lambda_0$ to $0.48\lambda_0$ and $0.462\lambda_0$ to $0.474\lambda_0$ with Kerr fields. This controlled SPP waves may show significant applications in the field of spectroscopy and sensing technology, optical tweezers, nano-photonics, radiation guiding, transformation optics, plasmonster technology, and photovoltaic devices.

References

[1] Farmani A, Mir A and Sharifpour Z 2018 *Appl. Surf. Sci.* **453** 358
[2] Humayun K and Haneef M 2018 *Can. J. Phys.* **96** 98
[3] Humayun K, Haneef M and Bakhtawar 2018 *Chin. Phys. B* **27** 014201
[4] Pu M, Yao N, Hu C, Xin X, Zhao Z, Wang C and Luo X 2010 *Opt. Express* **18** 21030
[5] Humayun K and Haneef M 2017 *Laser Phys.* **27** 055201
[6] Haneef M, Mohammad S, Akbar J, Arif S, Zahir M and Humayun K 2012 *Chin. Phys. Lett.* **29** 073201
[7] Rahman A, Ahmad I, Afaq A and Haneef M 2011 *Chin. Phys. Lett.* **28** 063301
[8] Farmani A, Yavarian M, Alighanbari A, Miri M and Sheikhi M H 2017 *Appl. Opt.* **56** 8931
[9] Pines D 1956 *Rev. Mod. Phys.* **28** 184
[10] Wood R W 1902 *Philos. Mag.* **4** 396
[11] Ritchie R H 1957 *Phys. Rev.* **106** 874
[12] Zayatsa A V, Smolyaninovb I I and Alexei A 2005 *Phys. Rep.* **408** 131
[13] Gramotnev D K and Bozhevolnyi S I 2010 *Nat. Photonics* **4** 83
[14] Haynes C L, McFarl A D and VanDuyne R P 2005 *Anal. Chem.* **77** 338A
[15] Agranovich V M and Mills D L 1982 *Surface Polaritons — Electromagnetic Waves at Surfaces and Interfaces* (Amsterdam: North-Holland)
[16] Raether H 1988 *Surface Plasmons on Smooth and Rough Surfaces and on Gratings* (Berlin: Springer-Verlag)
[17] Boardman A D 1982 *Electromagnetic Surface Modes* (New York: Wiley)
[18] Boisde G and Harmer A 1996 *Chemical and Biochemical Sensing with Optical Fibers and Waveguides* (Boston: Arthech House)
[19] Ponath H E and Stegeman G I 1991 *Nonlinear Surface Electromagnetic Phenomena* (Amsterdam: North-Holland)
[20] Qin C, Xiaohua S, Yong M and Jin H 2012 *Plasmonics* (Chap. 20) (Kim K Y Ed.) (Croatia: InTech)
[21] Pohl D W and Courjon D 1993 *Near Field Optics* (Netherlands: Kluwer)
[22] Reddick R C, Warmack R. J and Ferrel T L 1989 *Phys. Rev. B* **39** 767
[23] Courjon D, Sarayeddine K and Spajer M 1989 *Opt. Commun.* **71** 23
[24] Fornel F D, Goudonnet J P, Salomon L and Lesniewska E 1989 *Proc. SPIE* **1139** 77
[25] Marti O, Bielefeldt H, Hecht B, Herminhaus S, Leiderer P and Mlynek J 1993 *Opt. Commun.* **96** 225
[26] Adam P M, Salomon L, Fornel F D and Goudonnet J P 1993 *Phys. Rev. B* **48** 2680
[27] Dawson P, Fornel F D and Goudonnet J P 1994 *Phys. Rev. Lett.* **72** 2927
[28] Tsai D P, Kovasc J, Wang Z, Moskovits M, Shalaev V M, Suh J S and Botet R 1994 *Phys. Rev. Lett.* **72** 1994
[29] Bozhevolnyi S I, Smolyaninov I I and Zayats A V 1995 *Phys. Rev. B* **51** 17916
[30] Minovich A E, Miroshnichenko A E, Bykov A Y, Murzina T V, Neshev D N and Kivshar Y S 2015 *Laser Photonics Rev.* **9** 195
[31] Keren-Zur S, Avayu O, Michaeli L and Ellenbogen T 2015 *ACS Photonics* **3** 117
[32] Almeida E, Shalem G and Prior Y 2016 *Nat. Commun.* **7** 10367
[33] Lee J, Tymchenko M, Argyropoulos C, Chen P Y, Lu F, Demmerle F, Boehm G, Amann M C, Alu A and Belkin M A 2014 *Nature* **511** 65
[34] Nookala N, Lee J, Tymchenko M, Gomez-Diaz J S, Demmerle F, Boehm G, Lai K, Shvets G, Amann M C, Alu A and Belkin M 2016 *Optica* **3** 283
[35] Kelley P L 1965 *Phys. Rev. Lett.* **15** 1005
[36] Zel'dovich B Y, Pilipetsky N F and Shkunov V V 1985 *Principles of Phase Conjugation* (Berlin: Springer-Verlag)
[37] Gibbs M H, McCall L S and Venkatesan C N T 1976 *Phys. Rev. Lett.* **36** 1135
[38] Silberberg Y and Joseph I B 1982 *Phys. Rev. Lett.* **48** 1541
[39] Sahraia M, Hamedia H R and Memarzadeha M 2012 *J. Mod. Opt.* **59** 980
[40] Schmidt H and Imomoglu A 1996 *Opt. Lett.* **21** 1936
[41] Bacha B A, Ghafoor F, Ahmad I and Rahman A 2014 *Laser Phys.* **24** 055401
[42] Xiao Y, Qian H and Liu Z 2018 *ACS Photonics* **5** 1654
[43] Rokhsari H and Vahala K J 2005 *Opt. Lett.* **30** 427
[44] Bacha B A, Ghafoor F, Ahmad I and Rahman A 2014 *Laser Phys.* **24** 055401
[45] Ahmad S, Ahmad A, Bacha B A, Khan A A and AbdulJabar M S 2017 *Eur. Phys. J. Plus* **132** 506
[46] Krasnok A, Tymchenko M and Alù A 2017 *Mater. Today* **21** 8